A revisited adaptive super-twisting control of underactuated mechanical systems: Design and experiments

Afef Hfaiedh, Ahmed Chemori, Afef Abdelkrim

Journal Title
XX(X):2–28

DOI: 10.1177/ToBeAssigned
www.sagepub.com/
SAGE

A Revisited Adaptive Super-Twisting Control of Underactuated Mechanical Systems: Design and Experiments

Afef Hfaiedh[1] and Ahmed Chemori[2] and Afef Abdelkrim[1]

Abstract

In this study, a new robust control approach is proposed for class I of Underactuated Mechanical Systems (UMSs). UMSs have fewer actuators than degrees of freedom (DOFs) and are characterized by a nonlinear coupling between actuated and non-actuated coordinates. They are also characterized by the instability of internal dynamics, making control design a challenging task. Moreover, due to the loss of actuators, UMSs are more sensitive to parametric variations and external disturbances. To address these issues, we propose to design a revisited adaptive super-twisting (ASTW) control based on an explicit global change of coordinates. The proposed approach requires a few assumptions regarding system dynamics. Based on Lyapunov's theory, a stability analysis of the resulting closed-loop system was performed. Numerical simulations were conducted on the inertia wheel inverted pendulum, showing the robustness of the proposed adaptive control scheme toward constant uncertainties and disturbances dependent on both state and time. An experimental comparative study between the proposed approach and existing controllers was conducted to demonstrate the effectiveness of the proposed control strategy.

Keywords

Underactuated Mechanical systems, Robust Control, Strict-Feedback form, Lyapunov analysis, Inertia Wheel Inverted Pendulum.

Prepared using sagej.cls *[Version: 2017/01/17 v1.20]*

Introduction

Sliding mode control (SMC) is a well-known robust control widely used for nonlinear systems Utkin (1992) due to its robustness against matched uncertainties and disturbances. The first-order SMC is characterized by an undesirable finite frequency and amplitude oscillations around a predefined switching manifold, known as chattering phenomenon. From a practical point of view, the chattering involves high control activity by generating the high-frequency of non-modeled dynamics Slotine and Li (1991) and will result in unnecessary/rapid wear of the actuation components Andrzej (2000). The high-frequency oscillation can be caused, for instance, by the presence of a parasitic dynamics in series with the control system or by switching time delays. More details regarding the causes of this phenomenon are provided in Yu and Kaynak (2009). To overcome the chattering problem, various solutions include, but not limited to, continuous approximation of the discontinuous control law Slotine and Li (1991), observer-based approaches Bondarev et al. (1985), second-order sliding mode control Gonzalez et al. (2012), and intelligent approximation algorithms Nafa et al. (2021). The Super-Twisting Algorithm (STA) introduced in Levant (1993) is a second-order sliding mode controller that is a powerful tool for minimizing the effect of chattering. STA has shown promising results in terms of robustness and fast response. It has the ability to generate a continuous control signal, and is appropriate for systems with Lipschitz continuous matched uncertainties/disturbances with bounded gradients Ramesh-Kumar and Bandyopadhyay (2014). Various stability analysis techniques based on the Lyapunov theory have been proposed in the literature to ensure finite-time convergence with an estimation of the convergence time for unperturbed dynamics Sanchez and Moreno (2012), systems with perturbations dependent only on time Levant (1993) and systems with perturbations depending on both state and time Castillo et al. (2018). In addition, the super-twisting (STW) approach has been widely employed for controlling various underactuated mechanical systems (UMSs). A STW scheme, was designed in Sun et al. (2015) for a perturbed underactuated crane system. To define an optimal sliding surface for the STW controller, an optimal controller was proposed in Ramos-Paz et al. (2017) to control an underactuated pendubot system. A smooth STW control scheme

[1]University of Carthage, National Engineering School of Carthage (ENICarthage), LR18ES44 Research Laboratory Smart Electricity & ICT, SE&ICT Lab, Tunis, Tunisia
[2]LIRMM, University of Montpellier, CNRS, Montpellier, France

Corresponding author:
Afef Hfaiedh University of Carthage, National Engineering School of Carthage (ENICarthage), LR18ES44 Research Laboratory Smart Electricity & ICT, SE&ICT Lab, Tunis, Tunisia
Email: afef.hfaiedh@enicar.u-carthage.tn

Prepared using sagej.cls

was proposed in Din et al. (2018) to control a beam-and-ball system based on the transformation of system dynamics in a canonical form. An STW -based-disturbance observer was proposed in Hfaiedh et al. (2020a). Recently, several research efforts have been made to address modelling, stability, and control issues of nonlinear second-order UMSs Krafes et al. (2018). In Nafa et al. (2021), an adaptive controller using sliding mode control (SMC) and a wavelet network (WN) was proposed for a class of second-order UMSs with two DOFs. Theoretical and numerical analyses demonstrated that the proposed approach ensures the asymptotic stability and convergence of the closed-loop system. In Lu and Fang (2021) a gain-adapting coupling controller was designed by incorporating several unactuated state-related information into the control law. A real-time comparative study with a PID controller was performed to demonstrate the efficiency of the proposed method. In Hfaiedh and Abdelkrim (2022) another real-time implementation of an adaptive sliding mode control was proposed, where the switching gain was dynamically estimated using adaptive laws. It is based on the approximation of the signum function using a hyperbolic tangent function. The main drawback of this control approach lies in the chattering, which still represents the main issue for the SMC in terms of real-time implementation. Various existing works can also be found in the literature, based on adaptive control Roy et al. (2021), feedback robust integral of the sign of the error (RISE) control Hfaiedh et al. (2021), third-order discontinuous integral algorithm Gutiérrez-Oribio et al. (2021), interconnection and damping assignment-passivity-based control (IDA-PBC) approaches Gritli et al. (2017) Hfaiedh et al. (2020b) and passivity-based approaches Zhai et al. (2022). Other intelligent algorithms used to improve robustness and capture unknown dynamics of underactuated systems with constraints were proposed in Yang et al. (2023) Yang et al. (2021). These algorithms are designed to learn from training and can adapt to changing system dynamics; however, they may require a large amount of data to train and specific hardware architectures to be implemented.

In this study, we focus on the control problem of nonlinear second-order UMSs, while dealing with external disturbances, parametric uncertainties, and perturbations depending on both states and time. The proposed control solution is an ASTW algorithm, based on collocated partial feedback linearization, validated through real-time experiments on the IWIP, and compared to other existing methods from the literature.

ASTW control has already been used in the literature to control fully actuated systems Shtessel et al. (2012) Rajappa et al. (2016). However, it is not straightforwardly applicable to UMSs because of(i) underactuation, which represents a source of dynamic constraints; (ii) the complexity and diversity of the nonlinear coupling between coordinates, which differs from one system to another; (iii) their nonlinear dynamics; (iv) their unstable internal dynamics; (v) external disturbances; and (vi) parametric uncertainties.

For fully actuated systems, the system can be directly controlled and the control problem is often well-defined; however, for UMSs, the control problem involves designing a controller that can exploit

the inherent dynamics of the system to achieve the desired output behavior. Nevertheless, it is possible to indirectly control the coordinates of the internal dynamics using appropriate techniques. Control design is intended to allow such systems to perform complex tasks with fewer actuators. If the aforementioned aspects are not considered in the control design, the system will fail to provide the intended response, which may result in instability or degraded performance of the control system. In summary, to address the aforementioned aspects, the main contributions of this study are summarized below:

1. **Nonlinear coupling between coordinates**: We propose to transform the system into a strict-feedback form in order to decouple the system into (inner nonlinear and linear subsystems).
2. **Instability of internal dynamics**: We propose two new desired trajectories, required for the design of the sliding surface. The choice behind the desired trajectory is based on the asymptotic stability of the internal dynamics represented by the nonlinear subsystem.
3. **Uncertainties and external disturbances inherent to real applications**: We propose to benefit from the advantages of the STW with the important feature of the adaptation law to guarantee the establishment of a real second-sliding mode, despite the presence of parametric uncertainties and state and time dependent disturbances. Furthermore, it is worth noting that the proposed controller is appropriate for the case in which the bounds of the uncertainties and perturbations are unknown and cannot be estimated for real applications. It does not require any information regarding the bounds of disturbances and their gradients, except for their existence.
4. **Theoretical closed-loop stability analysis**: The stability analysis of the whole resulting closed-loop system is provided based on Lyapunov theory.
5. **Validation**: To validate the proposed developments, simulation and experimental comparative studies between SMC, STW, RISE, and the proposed ASTW controllers were conducted on the testbed of the IWIP, where several scenarios were considered to demonstrate the effectiveness and robustness of the proposed controller, as well as its superiority with respect to state-of-the-art methods.

The rest of the paper is organized as follows: Section II presents a brief background on class I UMSs. Section III presents a brief review of the super-twisting and adaptive super-twisting controllers. Section IV describes the application of the proposed approach to the testbed of the IWIP. Section V discusses the simulation results, and section VI presents the real-time experimental results. The conclusion and future directions are summarized in Section VII.

Class I of underactuated mechanical systems

Using an invertible change of control, underactuated mechanical systems with two degrees of freedom and one control input can be partially linearized by collocated partial-feedback linearization.

Collocated Partial Feedback Linearization

The Euler-Lagrange equations of motion of a UMS, with n configuration variables and m control inputs, can be written in the form: $\frac{d}{dt}(\frac{\partial L}{\partial \dot{q}}) - \frac{\partial L}{\partial q} = F(q)\tau$, where L is the Lagrangian, q denotes the generalized coordinates, $F(q) \in \mathbb{R}^{n\times m}$ is a full-column rank non-square matrix of the distribution of control inputs on the DOFs with $m < n$, $\tau \in \mathbb{R}^m$ denotes the control input vector. The general matrix form of the equation of motion for a UMS can be expressed as follows:

$$M(q)\ddot{q} + C(q,\dot{q})\dot{q} + G(q) = \mathbf{F(q)}\boldsymbol{\tau} \tag{1}$$

where $M(q)$ is the inertia matrix, $C(q,\dot{q})$ denotes the Coriolis and centrifugal force matrix, and $G(q)$ represents the gravity vector, τ is the control input vector. Variables q, $\dot{q}$ and $\ddot{q}$ denote the position, velocity, and acceleration vectors, respectively. Consider $F(q) = [0, I_m]^T$, and the first configuration variable $q_1 \in \mathbb{R}^{n-m}$ is the unactuated coordinate and the second configuration variable $q_2 \in \mathbb{R}^m$ represents the actuated coordinate. The dynamics of a second-order UMS ($m = 1, n = 2$) is expressed in the following form:

$$\begin{bmatrix} m_{11} & m_{12} \\ m_{21} & m_{22} \end{bmatrix} \begin{bmatrix} \ddot{q}_1 \\ \ddot{q}_2 \end{bmatrix} + \begin{bmatrix} h_1(q,\dot{q}) \\ h_2(q,\dot{q}) \end{bmatrix} = \begin{bmatrix} 0 \\ \tau \end{bmatrix} \tag{2}$$

where m_{ij} i, for $j = 1,2$ represent the inertial terms. $h_i(q,\dot{q})$ for $i = 1,2$ include the Coriolis, centrifugal, and gravity terms.

In this study, we adopted the method of partial feedback linearization proposed in Spong (1994), where the system (2) is partially linearized.

Lemma 1: Consider a global invertible change of control of the form $\tau = \Theta(q)u + \Upsilon(q,\dot{q})$, for which the dynamics (2) is partially linearized as follows:

$$\begin{aligned} \dot{q}_1 &= p_1 \\ \dot{p}_1 &= f_0(q,p) + g_0(q)u \\ \dot{q}_2 &= p_2 \\ \dot{p}_2 &= u \end{aligned} \tag{3}$$

where $x = [q_1, p_1, q_2, p_2]^T$ is the new state vector after partial linearization, $f_0(q,p)$ and $g_0(q)$ are expressed by $f_0(q,p) = -m_{11}^{-1}(h_1(q,\dot{q}))$ and $g_0(q) = -m_{11}^{-1}(q)m_{12}(q)$. The expressions for $\Theta(q)$ and $\Upsilon(q,\dot{q})$ of the invertible change of control are described by $\Theta(q) = m_{22}(q) - m_{21}(q)m_{11}^{-1}(q)m_{12}(q)$ and $\Upsilon(q,\dot{q}) = h_2(q,\dot{q}) - m_{21}m_{11}^{-1}(q)h_1(q,\dot{q})$.

After the partial feedback linearization, the system is represented in the form of two subsystems. The control input u appears in both the nonlinear (q_1, p_1)- and the linear (q_2, p_2)-subsystems. These two subsystems can be decoupled through a global change of coordinates. This transformation is described in detail in the next section.

Strict-feedback form

The explicit change of coordinates were determined, which, from the partial feedback linearization of Spong and Praly (1997), transforms the system (3) into a strict-feedback representation, where the control input appears only in the linear subsystem Olfati-Saber (2001). This change in coordinates is expressed as follows:

$$\begin{aligned} z_1 &= q_1 + \gamma(q_2) \\ z_2 &= m_{11}(q_2)p_1 + m_{12}(q_2)p_2 \\ \xi_1 &= q_2 \\ \xi_2 &= p_2 \end{aligned} \tag{4}$$

where $\gamma(q_2) = \int_0^{q_2} m_{11}^{(-1)}(\theta)m_{12}(\theta)d\theta$ and $x_z = [z_1, z_2, \xi_1, \xi_2]^T$ denotes the state vector of the new representation. Using these new states, a new representation of the system composed of a linear (double integrator) subsystem and a nonlinear core subsystem was obtained Olfati-Saber (2001). The new system representation is described as follows:

$$\begin{aligned} \dot{z}_1 &= m_{11}^{-1}(\xi_1)z_2 \\ \dot{z}_2 &= g_1(z_1 - \gamma(\xi_1), \xi_1) \\ \dot{\xi}_1 &= \xi_2 \\ \dot{\xi}_2 &= u \end{aligned} \tag{5}$$

where $g_1(q_1, q_2) = -\frac{\partial V_p(q)}{\partial q_1}$, $V_p(q)$ denotes the potential energy of the system, and u denotes the control input obtained based on the collocated partial feedback linearization Spong (1994).

To sum up, the dynamics of (2) belongs to the Class I of UMSs based on the classification of Olfati-Saber (2001). By changing the control, the dynamics (2) were partially linearized to obtain the normal

form (3). Through a global change in coordinates, (3) is decoupled and transformed into a strict-feedback representation (5).

Remark 1. *Without loss of generality, the proposed approach can easily be generalized to other systems of class I, such as the translational oscillator with rotational actuator (TORA) and Acrobot. Furthermore, it can be extended to higher-order systems that can be transformed into a strict feedback form, such as the vertical take-off and landing aircraft Olfati-Saber (2001).*

Remark 2. *A system may be controllable but still not stabilizable for various reasons such, as unmeasurable states. To address these issues in underactuated systems, we propose to use the partial-feedback linearization to transform the system into a controllable and stabilizable form and design a control law to achieve the desired performance.*

In the following section, an ASTW scheme is proposed for a second-order UMS, and the stability analysis is addressed using Lyapunov's theory.

Control design

After the transformation of the equation of motion (1) into a strict feedback form, a sliding mode controller was designed in the presence of bounded disturbances for the single-input cascade nonlinear system (5).

A brief background on Super-Twisting SMC

Consider that the dynamics (5) has the general form $\dot{x} = f(x) + g(x)u$, where f and g are nonlinear functions and u is the control input. The STW control law Moreno and Osorio (2008) can be described as follows:

$$u = -k_1|\sigma|^{\frac{1}{2}} sign(\sigma) + w \tag{6}$$

$$\dot{w} = -k_2 sign(\sigma) \tag{7}$$

where σ is the sliding variable, and k_1 and k_2 are positive constant design gains. Now, considering an uncertain nonlinear scalar system Rivera et al. (2011):

$$\dot{\sigma} = f(t,\sigma) + u \tag{8}$$

where u is the control input (6) and the function $f(t,\sigma)$ is a perturbation term globally bounded as follows: $f(t,\sigma) \leq \delta|\sigma|^{\frac{1}{2}}$, for some positive constant $\delta > 0$. The closed-loop system resulting from

replacing (6)-(7) in (8) is expressed as:

$$\dot{\sigma} = -k_1|\sigma|^{\frac{1}{2}}sign(\sigma) + w + f(t,\sigma) \tag{9}$$

$$\dot{w} = -k_2 sign(\sigma) \tag{10}$$

For stability analysis, let us consider the vector $\zeta^T = [\zeta_1, \zeta_2]^T = [|\sigma|^{\frac{1}{2}}sign(\sigma), w]^T$ and propose the following quadratic Lyapunov candidate:

$$V = 2k_2|\sigma| + \frac{1}{2}w^2 + \frac{1}{2}(k_1|\sigma|^{\frac{1}{2}}sign(\sigma) - w)^2 \tag{11}$$

$$= \zeta^T P \zeta \tag{12}$$

where P is a positive, symmetric matrix given by $P = \frac{1}{2}\begin{pmatrix} 4k_2 + k_1^2 & -k_1 \\ -k_1 & 2 \end{pmatrix}$.

Remark 3. *It is worth noting that $V(x)$ appears to be discontinuous because it contains the term $sign(\sigma)$; however, it can be considered a continuous function everywhere, except at $x_1 = 0$, where it is not differentiable Moreno and Osorio (2008).*

The time derivative of the Lyapunov function (11) along the solutions of the system (9) leads to the following:

$$\dot{V} = -\frac{k_1 \zeta^T Q \zeta}{2\sqrt{|\sigma|}} \tag{13}$$

where $\mathbf{Q} = \begin{pmatrix} 2k_2 + k_1^2 - (\frac{4k_2}{k_1} + k_1)\delta & -k_1 + 2\delta \\ -k_1 + 2\delta & 1 \end{pmatrix}$.
It is worth noting that $\dot{V}$ is negative definite for any $Q > 0$ and k_1 and k_2 chosen such that: $k_1 > 2\delta$ and $k_2 > k_1 \frac{5\delta k_1 + 4\delta^2}{2(k_1 - 2\delta)}$.

Proposed adaptive super-twisting controller

The system (5) may be reformulated in the general form $\dot{x} = F(x,t) + G(x)u$, where $u \in \mathbb{R}$ is the control input and $x \in \mathbb{R}^n$ is the state vector.

Assumption 1: The sliding dynamics of the system (5) described in the form $\dot{x} = F(x,t) + G(x)u$, represents an uncertain nonlinear system that can be expressed as follows:

$$\dot{\sigma} = \Psi(x,t) + \Phi(x,t)u \tag{14}$$

where $\Psi(x,t) = \frac{\partial \sigma}{\partial t} + \frac{\partial \sigma}{\partial x} F(x,t)$ and $\Phi(x,t) = \frac{\partial \sigma}{\partial x} G(x)u$. Furthermore, assume that the function $\Phi \in \mathbb{R}$ can be expressed as a sum of a known function Φ_0 and a bounded perturbation $\Delta\Phi$ with unknown boundaries:

$$\Phi(x,t) = \Phi_0(x,t) + \Delta\Phi(x,t) \tag{15}$$

where $\frac{|\Delta\Phi|}{\Phi_0} \leq \varphi_1 < 1$.

Assumption 2: The function Ψ can be expressed as a sum of two bounded terms:

$$\Psi(x,t) = \Psi_1(x,t) + \Psi_2(x,t) \tag{16}$$

Suppose that $\delta_1, \delta_2 > 0$ exist but are not known, therefore $|\Psi_1(x,t)|$ and $\Psi_2(x,t)$ can be bounded as follows:

$$\begin{aligned} |\Psi_1(x,t)| &\leq \delta_1 |\sigma|^{\frac{1}{2}} \\ \dot{\Psi}_2(x,t) &\leq \delta_2 \end{aligned} \tag{17}$$

Assumption 3: The system (14) can be rewritten in the following form:

$$\dot{\sigma} = \Psi + (1 + \frac{\Delta\Phi}{\Phi_0})\Phi_0 u \tag{18}$$

The function $\Phi_1 = (1 + \frac{\Delta\Phi}{\Phi_0})$ is bounded, that is:

$$1 - \varphi_1 \leq (1 + \frac{\Delta\Phi}{\Phi_0}) \leq 1 + \varphi_1 \tag{19}$$

Remark 4. *The main goal of the control law is to drive σ and $\dot{\sigma}$ to zero in the presence of the bounded perturbations considered in (15) and (17).*

Assumptions about the unknown and unmodeled parts in the system's dynamics have already been reported in the literature Shtessel et al. (2012). Bounded uncertainties can arise from a variety of sources, such as modeling errors, measurement noise, and external disturbances. If the system is subject to bounded perturbations with unknown boundaries, as stated in those assumptions, its inputs or parameters can vary within an unknown range of values. In this case, it is important to develop adaptive-based control strategies using online estimation techniques to handle the uncertainty and ensure stable and satisfactory performance. In addition, the perturbations can depend on both state and time. They are often the most challenging to handle in control systems because they can lead to highly complex and unpredictable

system behavior. The effect of the perturbation on the system can also vary depending on the current state of the system as well as how the perturbation changes over time.

Remark 5. *The ASTW controller was designed for fully actuated systems, as in Shtessel et al. (2012) for an electro-pneumatic actuator and in Rajappa et al. (2016) for a quadrotor UAV. This control scheme was also applied to a floating wind turbine in Zhang and Plestan (2021). It produces a continuous control signal, enabling the maintenance of control accuracy in the presence of perturbations and uncertainties, even if the system model knowledge is limited. However, to the best of our knowledge, this controller has never been generalized to the challenging case of control of UMSs.*

In this study, we considered the extension of this controller to the challenging case of class I UMSs described by the form (5), while considering unknown bounds of uncertainties and perturbations. In the next section, the design of the proposed controller is illustrated on a second-order UMS, and the stability analysis is addressed using the Lyapunov theory.

Remark 6. *When the bounds of uncertainties and perturbations are known, the control problem can be resolved with a super-twisting controller Moreno and Osorio (2008) Castillo et al. (2018). However, in our case, the bounds of uncertainties and perturbations $\delta_1, \delta_2, \varphi_1$ are unknown and accordingly cannot be estimated, particularly for real-time systems.*

Considering that the bounds on the uncertainties and perturbations are unknown, and the functions $\Phi_1, \Psi_1(x,t), \Psi_2(x,t)$ satisfy Assumptions 1,2 and 3, the adaptive super-twisting control guarantees a non-overestimation of the control gains k_1 and k_2, and ensures in a finite time $t_F \leq \frac{2V(t_0)^{1/2}}{\eta_0}$ the establishment of a real second-sliding mode, with $|\sigma| \leq \eta_1$, $\eta_1 > \mu$, $|\dot{\sigma}| \leq \eta_2$ and $\eta_2 > 0 \; \forall t > t_F$. Then, we consider that the gains are time-varying and described by $k_1 = k_1(\sigma, \dot{\sigma}, t)$ and $k_2 = k_2(\sigma, \dot{\sigma}, t)$. These can be estimated online according to the adaptation law proposed in Shtessel et al. (2012). The first gain k_1 is adapted as follows:

$$\dot{k}_1 = \begin{cases} \omega_1 \sqrt{\frac{\gamma_1}{2}} sign(|\sigma| - \mu) & \text{if } k_1 > k_m \\ \eta & \text{if } k_1 \leq k_m \end{cases} \tag{20}$$

and the second gain k_2 varies proportionally to k_1, according to the following expression:

$$k_2 = 2\varepsilon k_1 \tag{21}$$

where

- ω_1, γ_1, ε and η are arbitrary positive constants and $k_1(0) > k_m$.
- k_m is a small positive parameter introduced in the control law to maintain the positive gains.
- μ is a positive constant that defines the boundary layer for the real sliding mode.

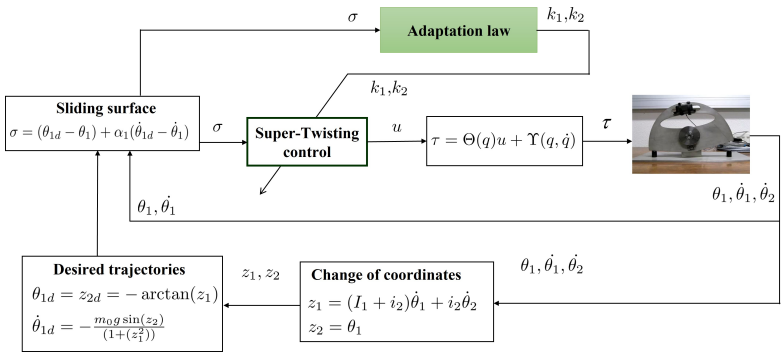

Figure 1. Schematic diagram of the proposed approach.

As mentioned in Rajappa et al. (2016), a wrong choice of the parameter μ could lead to either instability or overestimation of the control gains.

An illustrative application example

Underactuated mechanical systems are typically studied on a case-by-case basis. The proposed adaptive super-twisting control scheme for the general case of a Class I UMS is presented in this section. The entire bloc diagram of the designed approach is shown in Figure 1.

The inertia wheel inverted pendulum (IWIP)

In this study, an example of a system from Class I UMSs, namely the IWIP, was considered. This plant is an interesting typical benchmark, because with a reduced-order model, it inherits the same features of much more complex systems (e.g., human balance support devices Wojtara et al. (2012), gyrostabilizers, and stabilizers for self-balancing electric motorcycles Ho and Pham (2018)). It is characterized by two degrees of freedom and one control input. This system has attracted considerable interest from researchers. It was considered a benchmark for various recent studies, as in Gritli et al. (2017). The system includes an unactuated joint between the frame and pendulum body and an actuated joint between the body and inertia wheel, as illustrated in Figure 2.

The use of a simplified low-order system with the same features and basic functionality to address the common problems in high-order complex systems can be very useful. Low-order systems require fewer computational resources for simulations and a low cost for real-time experiments. They are often easier to use and understand the major control problems and challenges of high-order systems while enabling

experimental validation of the control design at an affordable cost in a laboratory (e.g., case of the IWIP), instead of an excessively high cost in real conditions (e.g., case of underwater vehicles).

The aim of the control problem was to design an ASTW algorithm to solve the stabilization problem of the system in the presence of unknown model uncertainties and external disturbances.
The dynamic model of the system can be computed following the Lagrange method. To this end, the Lagrangian of this system can be expressed by $L = \frac{1}{2}(I\dot{\theta}_1^2 + i_2(\dot{\theta}_1 + \dot{\theta}_2)^2) - m_0 g\cos(\theta_1)$ The application of the Lagrange equation leads to the following dynamic model:

$$\begin{bmatrix} I+i_2 & i_2 \\ i_2 & i_2 \end{bmatrix} \begin{bmatrix} \ddot{\theta}_1 \\ \ddot{\theta}_2 \end{bmatrix} - \begin{bmatrix} m_0 g\sin(\theta_1) \\ 0 \end{bmatrix} = \begin{bmatrix} 0 \\ \tau \end{bmatrix} \tag{22}$$

where $\theta = [\theta_1, \theta_2]^T$ is the vector of the generalized coordinates and τ is the torque generated by the actuator of the inertia wheel. The dynamic parameters of the system can be found in Hfaiedh et al. (2021) and Hfaiedh and Abdelkrim (2022). The parameters I and m_0 of the model are expressed by

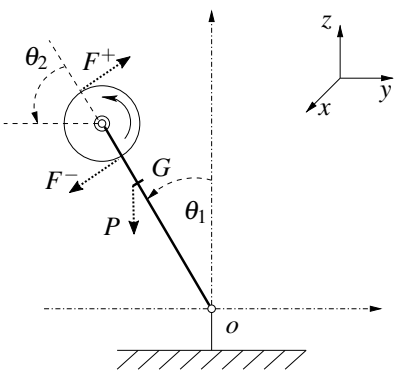

Figure 2. Schematic view of the system: the first joint θ_1 is unactuated, the second joint θ_2 is actuated.

$I = ml^2 + ML_1^2 + i_1$ and $m_0 = ml + ML_1$ respectively.

Control strategy

Using the method described in (5), the global change of coordinates is defined by: $z_1 = \frac{\partial L}{\partial \dot{\theta}_1} = (I+i_2)\dot{\theta}_1 + i_2\dot{\theta}_2$, $z_2 = \theta_1$, $z_3 = \dot{\theta}_2$, where $z = [z_1, z_2, z_3]^T$ denotes the state vector of the strict-feedback model. Using the Lagrangian formulation, the system is transformed into a cascade form as follows:

$$\dot{z}_1 = \frac{\partial L}{\partial \theta_1} = m_0 g\sin(z_2) \tag{23}$$

$$\dot{z}_2 = \frac{z_1}{I+i_2} - \frac{i_2 z_3}{I+i_2} \tag{24}$$

$$\dot{z}_3 = u \tag{25}$$

The resulting system is presented as a cascade connection between the linear and nonlinear subsystems Olfati-Saber (2001), where z_2 is considered as a virtual control input of the z_1 nonlinear subsystem. It is worth noting that because it does not play a significant role in the dynamic model and does not appear in the Lagrangian equation, the angular position of the inertial wheel is not considered as a state in the new model. Using a sigmoidal function $-\arctan(z_1)$ for z_2 in the z_1-subsystem can globally asymptotically stabilize (23), by choosing the Lyapunov function $V(z_1) = \frac{1}{2}z_1^2$. Let us now consider the desired trajectory and its time derivative, as follows:

$$\theta_{1d} = z_{2d} = -\arctan(z_1) \tag{26}$$

$$\dot{\theta}_{1d} = -\frac{m_0 g \sin(z_2)}{(1+(z_1^2))} \tag{27}$$

The time derivative of the Lyapunov function leads to the following:

$$\begin{aligned}
\dot{V}(z_1) &= z_1 \dot{z_1} \\
\dot{V}(z_1) &= z_1 m_0 g \sin(z_2) \\
\dot{V}(z_1) &= z_1 m_0 g \sin(-\arctan(z_1)) \\
\dot{V}(z_1) &= -z_1 m_0 g \frac{z_1}{\sqrt{1+z_1^2}}
\end{aligned} \tag{28}$$

It can be seen that (28) is negative definite by the choice of the desired trajectory (26) that globally asymptotically stabilizes $z1 = 0$. The stability analysis of the entire closed-loop system will be demonstrated in the sequel.

Let us now reconsider the control law (6)-(7) for the system (23-25) with adaptive feedback gains as follow:

$$u = -k_1(t)|\sigma|^{\frac{1}{2}} sign(\sigma) + w \tag{29}$$

$$\dot{w} = -k_2(t) sign(\sigma) \tag{30}$$

where the control feedback gains $k_1(t)$ and $k_2(t)$ are adapted from (20) and (21), respectively. Then consider the proposed sliding surface σ described as follows:

$$\sigma = (\theta_{1d} - \theta_1) + \alpha_1(\dot{\theta}_{1d} - \dot{\theta}_1) \tag{31}$$

Where θ_{1d} and $\dot{\theta}_{1d}$ are the desired pendulum angular position (26) and its first time-derivative (27), respectively, and α_1 is a positive constant gain.

By applying the time-derivative of the sliding surface (31), we obtain the expression of the sliding variable dynamics:

$$\dot{\sigma} = (\dot{\theta}_{1d} - \dot{\theta}_1) + \alpha_1(\ddot{\theta}_{1d} - \ddot{\theta}_1) \tag{32}$$

If we derive the expression of $\ddot{\theta}_1$ from (24) and (25), we obtain:

$$\ddot{\theta}_1 = -\frac{i_2}{I+i_2}u + \frac{m_0 g \sin z_2}{I+i_2} \tag{33}$$

Computing the time derivative of $\dot{\theta}_{1d}$, leads to:

$$\ddot{\theta}_{1d} = \frac{2m_0^2 g^2 z_1 \sin(z_2)^2}{(1+z_1^2)^2} - \frac{m_0 g \dot{z}_2 \cos(z_2)}{1+z_1^2} \tag{34}$$

Replacing (33) and (34) in (32) leads to the following system:

$$\dot{\sigma} = \Big[-\frac{m_0 g \sin(z_2)}{(1+(z_1^2))} - \dot{z}_2 \Big] + \alpha_1 \Big[\frac{2m_0^2 g^2 z_1 \sin(z_2)^2}{(1+z_1^2)^2} - \frac{m_0 g \dot{z}_2 \cos(z_2)}{1+z_1^2} + \frac{i_2}{I+i_2}u - \frac{m_0 g \sin(z_2)}{I+i_2} \Big] \tag{35}$$

By rearranging the terms, we obtain the following form:

$$\dot{\sigma} = \Psi(z) + \Phi u \tag{36}$$

Based on assumptions 1, 2, and 3, the control system (36) with (29) can be rewritten as follows:

$$\begin{aligned} \dot{\sigma} &= -k_1 \Phi_1 |\sigma|^{\frac{1}{2}} sign(\sigma) + \omega_0 + \Psi_1 \\ \dot{\omega}_0 &= -k_2 \Phi_1 sign(\sigma) + \dot{\Psi}_2 + \dot{\Phi}_1 w \\ \omega_0(0) &= 0 \end{aligned} \tag{37}$$

where $\Phi_1 = (1 + \frac{\Delta\Phi}{\Phi_0})$ and $\omega_0 = \Psi_2 + \Phi_1 w$. A new state vector $Z = [Z_1, Z_2]^T$ can be defined as:

$$Z = [Z_1, Z_2]^T = \Big[\ |\sigma|^{\frac{1}{2}} sign(\sigma), \quad \omega_0 \ \Big]^T \tag{38}$$

and accordingly, the system (37) can be rewritten as follows:

$$\begin{pmatrix} \dot{Z}_1 \\ \dot{Z}_2 \end{pmatrix} = \frac{1}{2|Z_1|} \begin{pmatrix} -\alpha\Phi_1 & 1 \\ -\beta\Phi_1 & 0 \end{pmatrix} \begin{pmatrix} Z_1 \\ Z_2 \end{pmatrix} + \frac{1}{2|Z_1|} \begin{pmatrix} 1 & 0 \\ 0 & 2|Z_1| \end{pmatrix} \begin{pmatrix} \Psi_1 \\ \dot{\hbar} \end{pmatrix} \tag{39}$$

where $\dot{\hbar} = \dot{\Psi}_2 + \dot{\Phi}_1 w$ and $\alpha = k_1$, $\beta = 2k_2$. Then, assume that $\Psi_1 = \rho_1 Z_1$ and $\dot{\hbar} = \frac{\rho_2}{2} sign(\sigma) = \frac{\rho_2}{2} \frac{Z_1}{|Z_1|}$, where $0 < \rho_1 < \delta_1$ and $0 < \rho_2 < \delta_5$, leads to:

$$\begin{pmatrix} \dot{Z}_1 \\ \dot{Z}_2 \end{pmatrix} = \frac{1}{2|Z_1|} \begin{pmatrix} -(\alpha\Phi_1 - \rho_1) & 1 \\ -(\beta\Phi_1 - \rho_2) & 0 \end{pmatrix} \begin{pmatrix} Z_1 \\ Z_2 \end{pmatrix} \tag{40}$$

$$\begin{pmatrix} \dot{Z}_1 \\ \dot{Z}_2 \end{pmatrix} = A(Z_1) \begin{pmatrix} Z_1 \\ Z_2 \end{pmatrix} \tag{41}$$

Now, let us consider the following Lyapunov function candidate Shtessel et al. (2012) for the system (41):

$$V(\mathbf{Z}, \alpha, \beta) = \mathbf{Z}^T P Z + \frac{1}{2\varphi_1}(\alpha - \alpha_*)^2 + \frac{1}{2\varphi_2}(\beta - \beta_*)^2 \tag{42}$$

where α_* and β_* are positive constants, and P is given by $P = \begin{bmatrix} \lambda + 4\varepsilon^2 & -2\varepsilon \\ -2\varepsilon & 1 \end{bmatrix}$. The positive definiteness of P is guaranteed for $\lambda > 0$. The first time-derivative of V leads to the following Shtessel et al. (2012):

$$\dot{V}(\mathbf{Z}, \alpha, \beta) = Z^T [A^T P + PA] Z + \frac{1}{\varphi_1}(\alpha - \alpha_*)\dot{\alpha} + \frac{1}{\varphi_2}(\beta - \beta_*)\dot{\beta} \tag{43}$$

where the first term is bounded as follows:

$$Z^T [A^T P + PA] Z \leq -\frac{1}{2|Z_1|} Z^T Q Z \tag{44}$$

where $Q = \begin{bmatrix} Q_1 & Q_3 \\ Q_3 & Q_4 \end{bmatrix} = \begin{bmatrix} 2\lambda\alpha\Phi_1 + 4\varepsilon\Phi_1(2\varepsilon\alpha - \beta) - 2(\lambda + 4\varepsilon^2)\rho_1 + 4\varepsilon\rho_2 & Q_3 \\ (\beta\Phi_1 - 2\varepsilon\alpha\Phi_1 - \lambda - 4\varepsilon^2) + 2\varepsilon\rho_1 - \rho_2 & 4\varepsilon \end{bmatrix}$.

If we assume that $\beta = 2\varepsilon\alpha$ and $\alpha > \frac{\delta_1(\lambda + 4\varepsilon^2) - \varepsilon(2\delta_5 + 1)}{\lambda(1 - \Phi_1} + \frac{(2\varepsilon\delta_1 - \delta_5 - \lambda - 4\varepsilon^2)^2}{12\varepsilon(1 - \Phi_1)}$, we guarantee that the matrix Q is positive definite.

Following the reasoning in Shtessel et al. (2012), it can be shown that the time derivative of V along the solutions of the system leads to the following:

$$\begin{aligned}\dot{V}(Z,\alpha,\beta) &= Z^T[A^TP+PA]Z+\frac{1}{\varphi_1}(\alpha-\alpha_*)\dot{\alpha}+\frac{1}{\varphi_2}(\beta-\beta_*)\dot{\beta} \\ &= \dot{Z}^TPZ+Z^TP\dot{Z}+\frac{1}{\varphi_1}(\alpha-\alpha_*)\dot{\alpha}+\frac{1}{\varphi_2}(\beta-\beta_*)\dot{\beta}\end{aligned} \tag{45}$$

$$\dot{V}(Z,\alpha,\beta) \leq -\frac{1}{|Z_1|}Z^TQZ+\frac{1}{\varphi_1}(\eta_\alpha)\dot{\alpha}+\frac{1}{\varphi_2}(\eta_\beta)\dot{\beta} \tag{46}$$

$$\dot{V}(Z,\alpha,\beta) \leq -r(Z^TPZ)^{\frac{1}{2}}+\frac{1}{\varphi_1}(\eta_\alpha)\dot{\alpha}+\frac{1}{\varphi_2}(\eta_\beta)\dot{\beta} \tag{47}$$

$$\dot{V}(Z,\alpha,\beta) \leq -\eta_0[V(Z,\alpha,\beta)]^{\frac{1}{2}}+\aleph \tag{48}$$

$$\text{with } \aleph = -|\eta_\alpha|(\frac{1}{\varphi_1}\dot{\alpha}-\Omega_1)-|\eta_\beta|(\frac{1}{\varphi_2}\dot{\beta}-\Omega_2) \tag{49}$$

where $\eta_\alpha = \alpha-\alpha_* < 0$ and $\eta_\beta = \beta-\beta_* < 0$. $r = \frac{\varepsilon\lambda_{min}^{\frac{1}{2}}(P)}{\lambda_{max}(P)}$, $\Omega_1 = \frac{\omega_1}{\sqrt{2}\varphi_1}$ and $\Omega_2 = \frac{\omega_2}{\sqrt{2}\varphi_2}$, $\eta_0 = Min(r,\omega_1,\omega_2)$.

The first time-derivative of $\beta = 2\varepsilon\alpha$, leads to $\dot{\beta} = 2\varepsilon\dot{\alpha}$. Altogether with $\varepsilon = \frac{\omega_2}{2\omega_1}\sqrt{\frac{\varphi_2}{\varphi_1}}$ replaced in $\aleph$, leads to $\aleph = 0$; accordingly, $\dot{V}$ can be reduced and upper bounded as follows:

$$\dot{V}(Z,\alpha,\beta) \leq -\eta_0\sqrt{[V(Z,\alpha,\beta)]} \tag{50}$$

Numerical simulation results

In this study, the control objective was to stabilize the IWIP around its unstable equilibrium point. Both the STW and ASTW approaches were implemented using MATLAB/SIMULINK software (MathWorks) . The following three main simulation scenarios are considered:

Scenario 1: *Nominal case.*

Scenario 2: *Robustness towards parametric uncertainties.*

Scenario 3: *State and time dependent disturbance-rejection.*

In addition, the following initial conditions for the ASTW approach were considered: $x_{ASTW}(0) = [\theta_1,\dot{\theta}_1,\dot{\theta}_2,w(0),K_1(0)] = [\pi/2,0,0,0,50]$ and $x_{STW}(0) = [\theta_1,\dot{\theta}_1,\dot{\theta}_2,w(0)] = [\pi/2,0,0,0]$ for the super-twisting controller.

Scenario 1: nominal case

In the first scenario, we considered two case studies.
In the first case showed the performance of the proposed ASTW controller for different values of the key parameters γ_1 and ω_1. The results obtained for this case are shown in Figure 3, including the evolution versus time of the states, control input, sliding variable and estimated gains. From the results, the best response was obtained for the case of ($\omega_1 = 105$, $\gamma_1 = 57$), compared to the other selected values of ω_1 and γ_1. These curves show the stabilization of the system states around the unstable equilibrium point $[\theta_1, \dot{\theta}_1, \dot{\theta}_2] = [0,0,0]$ within a short time interval. The generated control input torque remained within the admissible limits of the actuator and converged to a zero steady-state value once the equilibrium point was reached.

Remark 7. *The control input applied to the system is expressed as* $\tau = \Theta(q)u + \Upsilon(q,\dot{q})$ *(cf. Lemma 1), where u is the expression of the ASTW controller. In our case, the obtained value of* Θ *was a small constant equal to* 0.0092*. For this reason, gains* ω_1 *and* γ_1 *have been selected to obtain robust results.*

In the second case study, we have fixed the gains $\omega_1 = 105$ and $\gamma_1 = 57$ and simulate the behavior of the system for different values of μ and ε. The simulation results are presented in Figure 4. The best results were observed for the cases of ($\mu = 10^{-3}, \varepsilon = 10^{-2}$) and ($\mu = 10^{-3}, \varepsilon = 10^{-1}$). It is worth noting that the system becomes unstable for larger parameter values. Indeed, the wrong choice of these parameters can lead to instability of the system, as shown for the case of $\mu = 5, \varepsilon = 1$ and $\mu = 0.5, \varepsilon = 10^{-2}$.

Scenario 2: robustness towards parametric uncertainties

The second scenario aimed to study the robustness of the proposed control scheme. Indeed, it allows us to check whether the applied control can adapt to uncertainties in the system parameters, which may be due to modeling errors, sensor inaccuracies, frictional forces, or other external factors. We introduced an uncertainty Δ_I on the parameter I and an uncertainty Δ_{m_0} on the parameter m_0. The parameters are selected because they represent a combination of several dynamic parameters. The simulation results are presented in Figure 5. The proposed approach can compensate for these additive uncertainties even for a large percentages of $\Delta_I = 200\%$ and $\Delta_{m_0} = 200\%$, where the estimated parameters remain bounded. Further, if the considered uncertainty increases, the reaching time also increases.

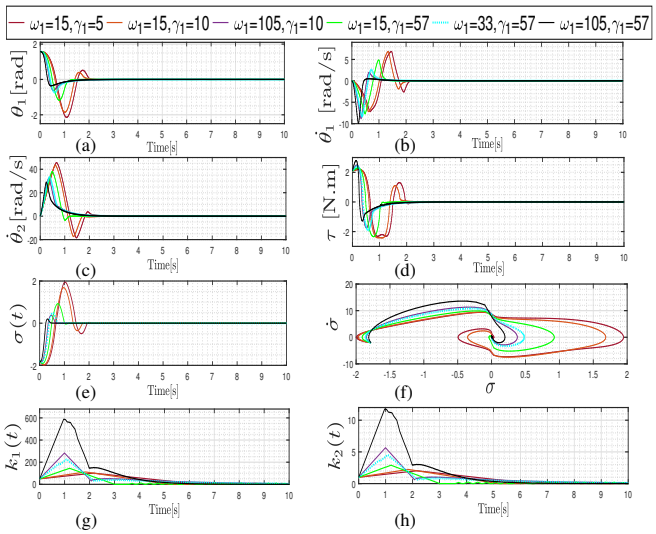

Figure 3. Obtained simulation results for scenario 1 **(case 1:** $\varepsilon = 10^{-2}, \mu = 10^{-4}, \eta = 0.1, k_m = 0.1$**)**. (a): Pendulum angular position , (b): pendulum angular velocity , (c): velocity of the inertia wheel , (d): the control input (torque), (e): the sliding variable, (f): the sliding diagram, (g): the estimated gain k_1, (h): the estimated gain k_2.

Scenario 3: external disturbances rejection

The main motivation behind the third scenario is to demonstrate the effectiveness of the proposed control scheme when the controlled system is subjected to state- and time-dependent disturbances. The applied disturbing signal for this case is expressed by $D = \frac{1}{1+(1500z_2)^2} + \frac{1}{1+(20\cos(t))^2}$, and was applied during the interval $[0, 60]$ seconds. The standard STW and the proposed ASTW controllers were compared. The selected design parameters used for the STW controller are set to $k_1 = 195$ and $k_2 = 2.43$. The simulation results for this scenario are presented in Figure 6. For clarity, the plots are zoomed, where we can clearly see the effect of the applied external disturbance on the evolution of the states in Figure 6(a-b-c) and the sliding variable σ in Figure 6(e) for the case of the STW controller.

However, based on the obtained results, we can notice that the proposed ASTW controller manages to compensate the applied external disturbance and brings back the states around the desired equilibrium point. The introduced external disturbance was compensated by the control action. A noticeable difference can be observed in the zoomed plots of the behavior of the STW and proposed ASTW controllers.

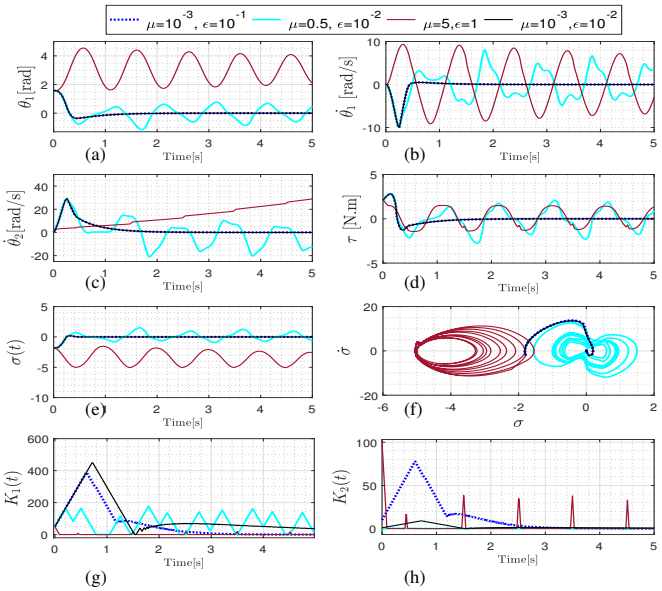

Figure 4. Obtained simulation results for scenario 1 **(case 2: $\omega_1 = 105$, $\gamma_1 = 57$)**. (a): Pendulum angular position , (b): pendulum angular velocity , (c): velocity of the inertia wheel , (d): the control input (torque),(e): the sliding variable, (f): the sliding diagram, (g): the estimated gain k_1, (h): the estimated gain k_2.

To sum up, the proposed ASTW controller provides better results than the standard STW controller and ensure a better compensation of time- and state-dependent disturbances.

Real-time experimental results

The experimental setup and some implementation issues are discussed in this section. Two experimental scenarios were conducted to validate the proposed control scheme. In the first scenario, no external disturbance is considered; however, the objective of the second scenario is to test the robustness of the proposed control scheme towards external disturbances. These scenarios tested the proposed controller under different dynamic operating conditions and compared its performance with that of other existing controllers from the literature. The results of each test are presented and discussed in this section.

Experimental setup and implementation issues

Real-time experiments were performed using an experimental testbed of the IWIP, as shown in Figure 7(a), and designed at LIRMM Laboratory Andary et al. (2009) Hfaiedh et al. (2018) Haddad et al.

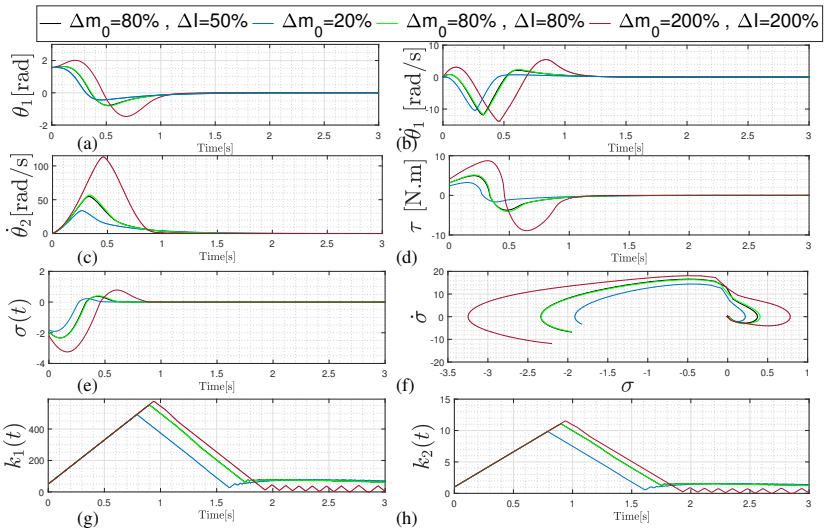

Figure 5. Obtained simulation results for scenario 2: (a): Pendulum angular position, (b): pendulum angular velocity, (c): velocity of the inertia wheel, (d): the control input (torque), (e): the sliding variable, (f): the sliding diagram, (g): the estimated gain k_1, (h): the estimated gain k_2.

(2018). The system is equipped with two sensors to measure the angular positions of the pendulum and the inertial wheel in real time. The angle of the inertial wheel was measured by an encoder mounted on its motor's shaft, and the pendulum body was equipped with an inclinometer to measure the pendulum's angle with respect to the vertical. Their corresponding velocities were calculated in real time by numerical derivatives. The entire system was supplied with a voltage equal to $12V$. Real-time communication and control were established by Ardence RTX OS with a sampling time of $6ms$. Two experiments were conducted to fairly compare the performance of the proposed ASTW scheme with existing controllers from the literature, including the (i) standard STW, (ii) first-order sliding mode (SMC) Hfaiedh and Abdelkrim (2022), and (iii) robust integral of the sign of the error (RISE) Hfaiedh et al. (2021) controllers. In the first scenario (nominal case), no external disturbances were considered. However, in the second case, we considered punctual external disturbances applied to the controlled systems. These disturbances were generated by a pendular system suspended from a fixed support, as illustrated in Figure 7. The same initial releasing position of the disturbing mass of the pendular system in Figure 7(b) were set for fair comparison. Accordingly, once the disturbing mass was launched, the same disturbing force F_{ext} at the impact position was approximately obtained.

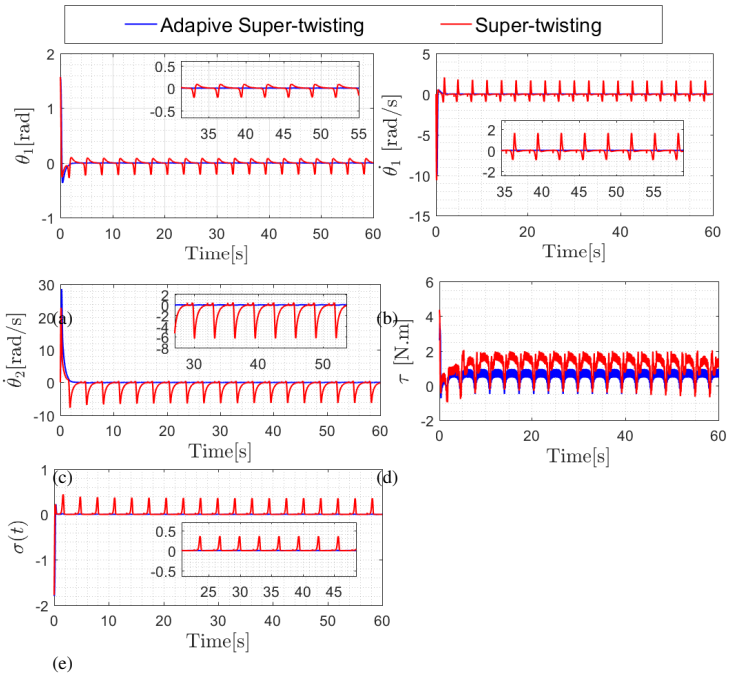

Figure 6. Obtained simulation results for scenario 3: External disturbances rejection. (a): Pendulum angular position versus time, (b): pendulum angular velocity versus time, (c): velocity of the inertia wheel versus time, (d): the control input τ versus time ,(e): Sliding variable versus time.

Performance evaluation criteria

To quantify the relevance of the control algorithms, we proposed computing the following criteria for all the implemented controllers.

The Integral Square Error (ISE):

$$ISE = \int e_{\theta_1}^2 dt \tag{51}$$

Integral Absolute Error (IAE):

$$IAE = \int |e_{\theta_1}| dt \tag{52}$$

where e_{θ_1} denotes the tracking error of the pendulum joint θ_1 with respect to its desired value (i.e., the equilibrium point).

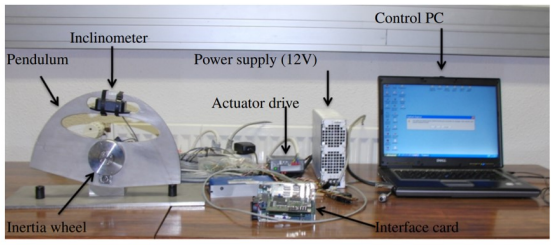

(a)

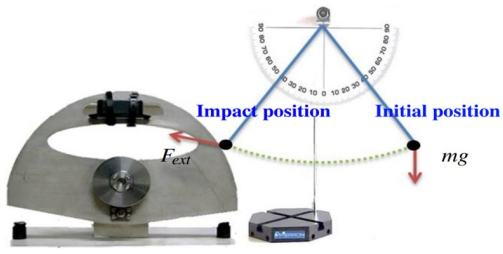

(b)

Figure 7. (a) View of the experimental setup of the IWIP and its main components, (b) Illustration of the punctual disturbances generator.

Parameters tuning

To select the adjustable gains in real tuning process, we started with small values to avoid any high and abrupt changes in the control input that may lead to a dangerous behavior or damage in the system's actuators. Subsequently, to obtain better performances, the parameters were progressively increased and the behavior of the closed-loop system was observed until the expected stabilization is reached. To sum up, the following 8-step algorithm is proposed:

Parameters' Tuning Algorithm

Step 1: Compute the expressions of Θ and Υ , taking into account the invertible change of control.

Step 2: Set the values of k_1 and k_m such that $k_1(0) > 1$ and $k_m = 1$.

Step 3: Initialization of ω_1, γ_1, ε and η with small values.

Step 4: Increase the value of $\Theta(q)$ until the pendulum is able to move from the initial condition.

Step 5: For fixed values of γ_1, ε and η, increase ω_1.

Step 6: For fixed values of ω_1 ,ε and η, increase γ_1.

Step 7: Set the values of ω_1 and γ_1 and increase the value of ε and η.

Step 8: Increase the value of k_m until obtaining a satisfactory behavior.

Experiment 1: Nominal case

In the first experiment, no external disturbance was considered. The following design parameters were used for the STW control scheme: $\alpha_1 = 0.057$, $K_2 = 0.00103$, $K_1 = 1.6$, $\Theta = 0.795$, $\Upsilon = 1.48 * \sin(\theta_1)$. The following design parameters were used for the ASTW control scheme: $\alpha_1 = 0.4$, $\gamma_1 = 5$, $\omega_1 = 20$, $\eta = 0.0010$, $\mu = 0.3382$, $K_m = 17.5$ and $\varepsilon = 0.1506$. For the RISE and SMC controllers, the design parameters were set as in Hfaiedh et al. (2021) and Hfaiedh and Abdelkrim (2022) respectively.
The obtained experimental results for all controllers are depicted in Figure 8. The convergence of state variables was established for all controllers. The state variables (Figure 8-(a,c,e)) in the case of the ASTW controller as well the control input (Figure 8-(b)) present less oscillations and ensure a faster convergence towards the equilibrium point than the standard STW, sliding mode and RISE controllers. The effectiveness of the proposed control scheme can also be observed in the phase profile shown in Figure 8-(d). More chattering in the voltage signal was observed for SMC than for the STW and proposed ASTW approaches (see the zoom plot in Figure 8-(f)).

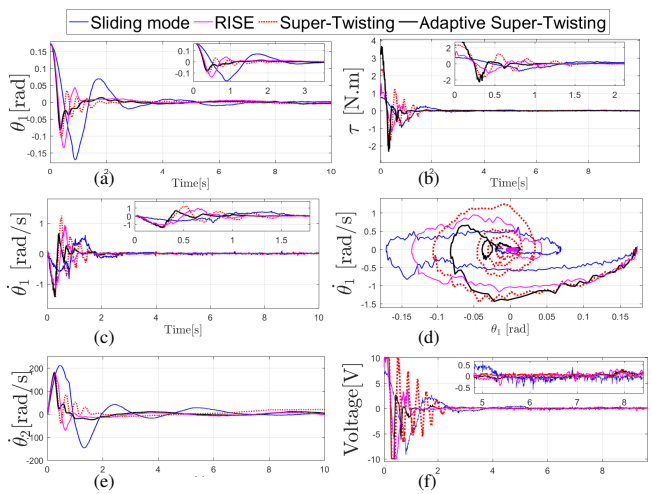

Figure 8. Obtained experimental results for scenario 1: Nominal case. (a): Pendulum angular position versus time, (b): Control Input versus time, (c): Pendulum angular velocity versus time ,(d): Phase diagram, (e): Velocity of the inertia wheel versus time, (f): Voltage control signal.

Experiment 2: External disturbances rejection

In this scenario, external disturbances were applied by the above-mentioned disturbances generator. An external disturbance was introduced at approximately $t_1 = 20s$. Throughout the experiments, we ensured that all controllers were subjected to identical disturbances. The experimental results are presented in Figure. 9. For a better view, the plots are magnified within the interval $[19, 23]$ s.

Both the proposed ASTW and the STW controllers reacted better to the applied disturbances than the RISE and SMC approaches and maintain the system around the desired equilibrium point as we can see in the evolution of the states and control signal. The exerted disturbance induces a high deviation from the desired equilibrium point of the pendulum angle position and velocity in the case of the first-order sliding mode controller, which results in poor behavior. However, the disturbance is better compensated by the proposed ASTW controller. More oscillations were observed in the standard STW control scheme. An improvement of the robustness of the proposed ASTW controller was observed when the controller compensated for the external punctual disturbance. These results were also confirmed by the proposed performance indices summarized in Table 1, where the improvement in the IAE and ISE criteria is recorded with respect to the SMC scheme. Similar improvements were obtained using the RISE and STW approaches. Better results were observed for the proposed ASTW controller. This result was obtained

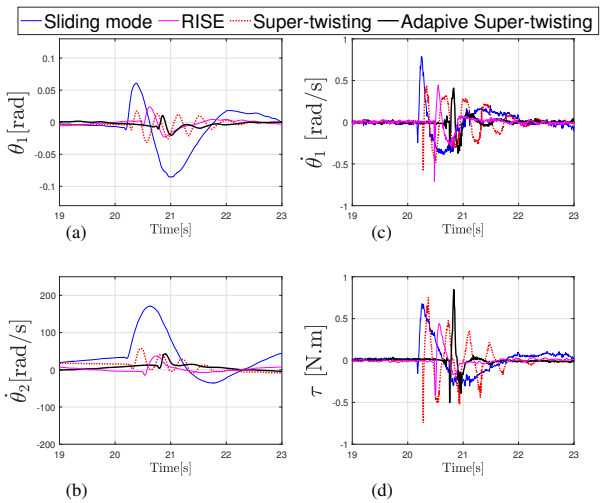

Figure 9. Obtained experimental results for scenario 2: Rejection of punctual external disturbances. (a): Pendulum angular position versus time, (b): Velocity of the inertia wheel versus time, (c): Pendulum angular velocity versus time,(d): Control Input versus time.

Table 1. Quantification of the performance through different evaluation criteria.

Criteria	SM	RISE	STW	ASTW
ISE	0.0043	$2.09e^{-4}$	$1.73e^{-4}$	$4.47e^{-6}$
Improvements		95.1395%	95.97%	99.8%
IAE	0.2127	0.0460	0.0422	0.0066
Improvements		78.37%	80.15%	96.8%

with respect to the standard sliding mode controller by computing the ISE of each controller. It is a performance metric used in control theory to evaluate the performance of a control system. It measures the square of the difference between the desired value and the actual output of the system and is integrated over a period of time. In our case we have only manipulated the unactuated coordinate as we are dealing with a stabilization problem around an unstable equilibrium point.

Conclusion and Future work

In this paper a revisited Adaptive Super-twisting Algorithm is proposed for class I UMSs. To define the sliding surface, two required desired trajectories were defined based on the transformation of the system into a strict-feedback form. The stability analysis of the resulting closed-loop system was proved using Lyapunov theory. Numerical simulations for different operating conditions (nominal and robustness towards uncertainties and state-/time- dependent disturbances) were conducted showing clearly the superiority of the proposed adaptive control approach with respect to STW algorithm. In addition, the obtained real-time experimental results, complied with some performance-evaluation criteria, clearly show that the proposed controller has significantly improved the performance of the system in terms of disturbance rejection compared with various existing controllers from the literature.

Future works may include the extension of the proposed control scheme with a prediction-based optimal gain selection of the super-twisting controller, as well as its generalization to other classes of underactuated mechanical systems with constraints.

References

Andary S, Chemori A and Krut S (2009) Control of the underactuated inertia wheel inverted pendulum for stable limit cycle generation. *Advanced Robotics* 23(15): 1999–2014. DOI:10.1163/016918609X12529279062438.

Andrzej B (2000) Chattering attenuation in sliding mode control systems. *Control and Cybernetics* 29: 585–594.

Bondarev A, Bondarev S, Kostyleva N and Utkin V (1985) Sliding modes in systems with asymptotic state observers. *Avtomat. i Telemekh (Autom. Remote Control)* 46(6): 679–684.

Castillo I, Fridman L and Moreno JA (2018) Super-twisting algorithm in presence of time and state dependent perturbations. *International Journal of Control* 91(11): 2535–2548. DOI:10.1080/00207179.2016.1269952.

Din S, Rehman F and Khan Q (2018) Smooth super-twisting sliding mode control for the class of underactuated systems. *PLoS One* 13(10).

Gonzalez T, Moreno J and Fridman L (2012) Variable gain super-twisting sliding mode control. *IEEE Transactions on Automatic Control* 57(8): 2100–2105. DOI:10.1109/TAC.2011.2179878.

Gritli H, Khraief N, Chemori A and Belghith S (2017) Self-generated limit cycle tracking of the underactuated inertia wheel inverted pendulum under IDA-PBC. *Nonlinear Dynamics* 89(3): 2195–2226. DOI:10.1007/s11071-017-3578-y.

Gutiérrez-Oribio D, Ángel Mercado-Uribe, Moreno JA and Fridman L (2021) Joint swing-up and stabilization of the reaction wheel pendulum using discontinuous integral algorithm. *Nonlinear Analysis: Hybrid Systems* 41: 101042. DOI:https://doi.org/10.1016/j.nahs.2021.101042.

Haddad NK, Chemori A and Belghith S (2018) Robustness enhancement of ida-pbc controller in stabilising the inertia wheel inverted pendulum: theory and real-time experiments. *International Journal of Control* 91(12): 2657–2672. DOI:10.1080/00207179.2017.1331378.

Hfaiedh A and Abdelkrim A (2022) Revisited adaptive sliding mode control of underactuated mechanical systems with real-time experiments. *International Journal of Modelling, Identification and Control* 37(3/4): 344 – 353. DOI:10.1504/IJMIC.2021.121848.

Hfaiedh A, Chemori A and Abdelkrim A (2018) Rise controller for class I of underactuated mechanical systems: Design and real-time experiments. In: *The 3rd International Conference on Electromechanical Engineering (ICEE'2018)*. Skikda, Algeria.

Hfaiedh A, Chemori A and Abdelkrim A (2020a) Disturbance observer-based super-twisting control for the inertia wheel inverted pendulum. In: *2020 17th International Multi-Conference on Systems, Signals Devices (SSD)*. pp. 747–752. DOI:10.1109/SSD49366.2020.9364233.

Hfaiedh A, Chemori A and Abdelkrim A (2020b) Stabilization of the inertia wheel inverted pendulum by advanced ida-pbc based controllers: Comparative study and real-time experiments. In: *2020 17th International Multi-Conference on Systems, Signals Devices (SSD)*. pp. 753–760. DOI:10.1109/SSD49366.2020.9364159.

Hfaiedh A, Chemori A and Abdelkrim A (2021) Observer-based robust integral of the sign of the error control of class i of underactuated mechanical systems: Theory and real-time experiments. *Transactions of the Institute of Measurement and Control* 44(2): 339–352. DOI:https://doi.org/10.1177/01423312211031396.

Ho QK and Pham CB (2018) Study on inertia wheel pendulum applied to self-balancing electric motorcycle. In: *2018 4th International Conference on Green Technology and Sustainable Development (GTSD)*. pp. 687–692. DOI:10.1109/GTSD.2018.8595698.

Krafes S, Chalh Z and Saka A (2018) A review on the control of second order underactuated mechanical systems. *Complexity* 2018: 17. DOI:10.1155/2018/9573514.

Levant A (1993) Sliding order and sliding accuracy in sliding mode control. *International Journal of Control* 58(6): 1247–1263. DOI:10.1080/00207179308923053.

Lu B and Fang Y (2021) Gain-adapting coupling control for a class of underactuated mechanical systems. *Automatica* 125: 109461.

Moreno JA and Osorio M (2008) A lyapunov approach to second-order sliding mode controllers and observers. In: *2008 47th IEEE Conference on Decision and Control*. pp. 2856–2861. DOI:10.1109/CDC.2008.4739356.

Nafa F, Boudouda I and Smaani B (2021) Adaptive wavelets sliding mode control for a class of second order underctuated mechanical systems. *Acta Polytechnica* 61(2): 350–363.

Olfati-Saber R (2001) *Nonlinear Control of Underactuated Mechanical Systems with Application to Robotics and Aerospace Vehicles*. PhD Thesis, Massachusetts Institute of Technology, Cambridge, MA, USA.

Rajappa S, Masone C, Bulthoff H and Stegagno P (2016) Adaptive super twisting controller for a quadrotor uav. In: *2016 IEEE International Conference on Robotics and Automation, ICRA 2016*, volume 2016-June. Stockholm, Sweden: Institute of Electrical and Electronics Engineers Inc., pp. 2971–2977. DOI:10.1109/ICRA.2016.7487462.

Ramesh-Kumar P and Bandyopadhyay B (2014) Variable gain super twisting controller for the position stabilization of stewart platform. *IFAC Proceedings Volumes* 47(1): 115 – 121. DOI:https://doi.org/10.3182/20140313-3-IN-3024.00189. 3rd International Conference on Advances in Control and Optimization of Dynamical Systems (2014).

Ramos-Paz S, Ornelas-Tellez F and Loukianov AG (2017) Nonlinear optimal tracking control in combination with sliding modes: Application to the pendubot. In: *2017 IEEE International Autumn Meeting on Power, Electronics and Computing (ROPEC)*. Ixtapa, Mexico, pp. 1–6. DOI:10.1109/ROPEC.2017.8261619.

Rivera J, Garcia L, Mora C, Raygoza JJ and Ortega S (2011) Super-twisting sliding mode in motion control systems. In: Bartoszewicz A (ed.) *Sliding Mode Control*, chapter 13. Rijeka: IntechOpen. DOI:10.5772/14532.

Roy S, Baldi S, Li P and Sankaranarayanan VN (2021) Artificial-delay adaptive control for underactuated euler–lagrange robotics. *IEEE/ASME Transactions on Mechatronics* 26(6): 3064–3075. DOI:10.1109/TMECH.2021.3052068.

Sanchez T and Moreno JA (2012) Construction of lyapunov functions for a class of higher order sliding modes algorithms. In: *In Proceedings of the 51st IEEE Conference on Decision and Control*. p. 6454–6459.

Shtessel Y, Taleb M and Plestan F (2012) A novel adaptive-gain supertwisting sliding mode controller: Methodology and application. *Automatica* 48(5): 759 – 769. DOI:https://doi.org/10.1016/j.automatica.2012.02.024.

Slotine J and Li W (1991) *Applied Nonlinear Control*. Prentice-Hall. ISBN 0130400491.

Spong M (1994) Partial feedback linearization of underactuated mechanical systems. In: *Proceedings of IEEE/RSJ International Conference on Intelligent Robots and Systems (IROS'94)*, volume 1. pp. 314–321 vol.1. DOI: 10.1109/IROS.1994.407375.

Spong MW and Praly L (1997) *Control of underactuated mechanical systems using switching and saturation*. Springer Berlin Heidelberg, pp. 162–172. DOI:10.1007/BFb0036093.

Sun N, Fang Y, Chen H and Fu Y (2015) Super-twisting-based antiswing control for underactuated double pendulum cranes. In: *2015 IEEE International Conference on Advanced Intelligent Mechatronics (AIM)*. Busan, South Korea, pp. 749–754. DOI:10.1109/AIM.2015.7222627.

Utkin V (1992) *Sliding Modes in Control and Optimization*. Springer-Verlag Berlin Heidelberg. ISBN 978-3-642-84379-2.

Wojtara T, Sasaki M, Konosu H, Yamashita M, Shimoda S, Alnajjar F and Kimura H (2012) Artificial balancer - supporting device for postural reflex. *Gait Posture* 35(2): 316–321.

Yang T, Sun N, Chen H and Fang Y (2023) Adaptive optimal motion control of uncertain underactuated mechatronic systems with actuator constraints. *IEEE/ASME Transactions on Mechatronics* 28(1): 210–222. DOI:10.1109/TMECH.2022.3192002.

Yang T, Sun N and Fang Y (2021) Neuroadaptive control for complicated underactuated systems with simultaneous output and velocity constraints exerted on both actuated and unactuated states. *IEEE Transactions on Neural Networks and Learning Systems* : 1–11DOI:10.1109/TNNLS.2021.3115960.

Yu X and Kaynak O (2009) Sliding-mode control with soft computing: A survey. *IEEE Transactions on Industrial Electronics* 56(9): 3275–3285. DOI:10.1109/TIE.2009.2027531.

Zhai M, Sun N, Yang T and Fang Y (2022) Underactuated mechanical systems with both actuator and actuated/unactuated state constraints: A predictive control-based approach. *IEEE/ASME Transactions on Mechatronics* : 1–13DOI:10.1109/TMECH.2022.3230244.

Zhang C and Plestan F (2021) Individual/collective blade pitch control of floating wind turbine based on adaptive second order sliding mode. *Ocean Engineering* 228: 108897. DOI:https://doi.org/10.1016/j.oceaneng.2021.108897.